Simulation of the High Frequency Hammer Peening Process for Improving the Fatigue Performance of Welded Joints

V. Hardenacke, M. Farajian, D. Siegele

Fraunhofer Institute for Mechanics of Materials IWM, Freiburg, Germany

Abstract

Post-treatment techniques like the high frequency hammer peening process exhibit a significant fatigue life enhancement of welded joints. The effectiveness of this mechanical impact treatment is primary based on three effects: The notch stress concentration at the weld toe is reduced, the local hardness is increased and compressive residual stresses are induced.

The goal of the present study was to develop a computationally efficient approach for predicting residual stresses induced by the hammer peening process on steel specimens. For that purpose, explicit simulations of the hammer peening post treatment process were performed utilizing the software package *ABAQUS*. Within the framework of the performed investigations, the suitability of different numerical features was analyzed.

The results of the simulations of the hammer peening process are in good agreement with experimental and analytical results, validating the reliability of the numerical approach. Furthermore, it is relatively straightforward to incorporate pre-existing residual stresses from welding and more complex specimen geometries in the model.

Keywords Welding, Residual Stresses, Fatigue Strength Improvement, Hammer Peening, Finite-Element Simulation.

Introduction

The innovation of locally modifying the residual stress state in welded components by the use of an ultrasonic hammering technology is widely attributed to E. Statnikov [1]. Nowadays, there are different hammer peening tool manufacturers and service providers, but the operating principle is always identical: an indenter is accelerated against a components surface with high frequency, causing local plastic deformation and residual stresses. The advantages of removing the potential threats of unwanted (tensile) residual stresses and exploiting the beneficial (compressive) residual stresses by mechanical treatments are already known in welding communities. In this context, high frequency hammer peening as post weld treatment is a statistically proven method to increase the fatigue life of welded joints [2-5]. During this process, a hardened cylindrical metal pin with a spherical tip impacts the weld toe surface with high frequency and induces local plastic deformation. The resulting compressive residual stresses, the reduced notch effect at the weld toe and the local work hardening of the material are the main reasons for the increased fatigue strength. Despite the successful practical application, a fundamental characterization of the governing formation mechanisms (with respect to the evolution of compressive residual stresses, work hardening and surface topography) on the material level is still missing. Thus, it must be assumed that due to the lack of experimental and numerical analyses of the high frequency hammer peening process the full potential of this proven post-treatment technique is not utilized.

Therefore, the goal of the present study was to develop a computationally efficient approach for predicting the residual stresses induced by the hammer peening process.

Numerical Studies

For all simulations a fully dynamic model was used (*ABAQUS EXPLICIT* solver). An explicit dynamic analysis is computationally efficient for the analysis of large models and allows for the definition of very general contact conditions.

The explicit dynamics analysis procedure is based upon the implementation of the explicit central-difference integration rule together with the use of diagonal element mass matrices (its inverse is simple to compute and the vector multiplication of the mass inverse by the inertial force requires only n operations, where n is the number of degrees of freedom in the model).

The explicit procedure integrates through time by using many small time increments. The central-difference operator is conditionally stable. An approximation for the stability limit is given by the smallest transit time of a dilatational wave across any of the elements in the mesh ($\Delta t \approx L_{min}/c_d$, where L_{min} is the smallest element length in the mesh and c_d is the dilatational wave speed). The use of small increments (dictated by the stability limit) is advantageous because it allows the solution to proceed without iterations and without requiring tangent stiffness matrices to be formed. It also simplifies the treatment of contact. In a three-dimensional analysis refining the mesh by a factor of two in each direction will increase the run time in the explicit procedure by a factor of sixteen (eight times as many elements and half the time increment size).

The simulation model for the numerical studies consists of sheet metal plate (specimen) with the dimensions 15*mm* x 4*mm* x 15*mm* and the hammer peening tool with a diameter of 4*mm* (at the tip). The specimen was modelled as elastic-plastic, while the hardened hammer peening tool was modelled as rigid. A contact pair was defined between the tool (master surface) and the specimen (slave surface), using a contact algorithm for the normal to surface direction (penalty or kinematic) and for the tangential direction (penalty). The hammering tool was upgraded using a connector element (contains elastic spring and dashpot). This upgrade enables the use of force controlled boundary conditions for the hammering tool [6].

Because only one hammering trace was considered, the problem was symmetric and only one half of the specimen had to be modelled (*y*-*z*-plane as the symmetry plane). The bottom side of the specimen was fixed by adequate displacement boundary conditions ($u_x=u_y=u_z=0$). Figure 1 (a) shows the complete FE-model.

The investigated numerical features include different hardening laws for the material, displacement and force controlled boundary conditions for the hardened metal pin, different degrees of mesh refinement and overlapping of indentations in the impact zone as well as a technique for a rapid mesh coarsening outside the hammer peening process zone.

The first investigated feature was the mesh refinement. The mesh spacing must be relatively fine at the impact zone and can coarsen towards the outer region. In the impact area, four degrees of mesh refinement were used. The very fine mesh features an element length of 100μm in the *x*-direction, 100μm in the *z*-direction and 50-85μm (biased, starting from specimen surface, ending at 1.25*mm* depth) in the *y*-direction. For the fine mesh the values are 125μm x 125μm x (75-135)μm, for the medium mesh 200μm x 200μm x (100-150)μm and for the coarse mesh 250μm x 200μm x (150-185)μm. In all cases the element type was *ABAQUS* C3D8R (8-node brick, tri-linear shape function, reduced integration). The residual stresses σ_{xx} were evaluated at paths in the middle of the specimen (*z*=7.5*mm* ± 0.5*mm*, the respective average values are shown in the following diagrams), see Figure 1 (b).

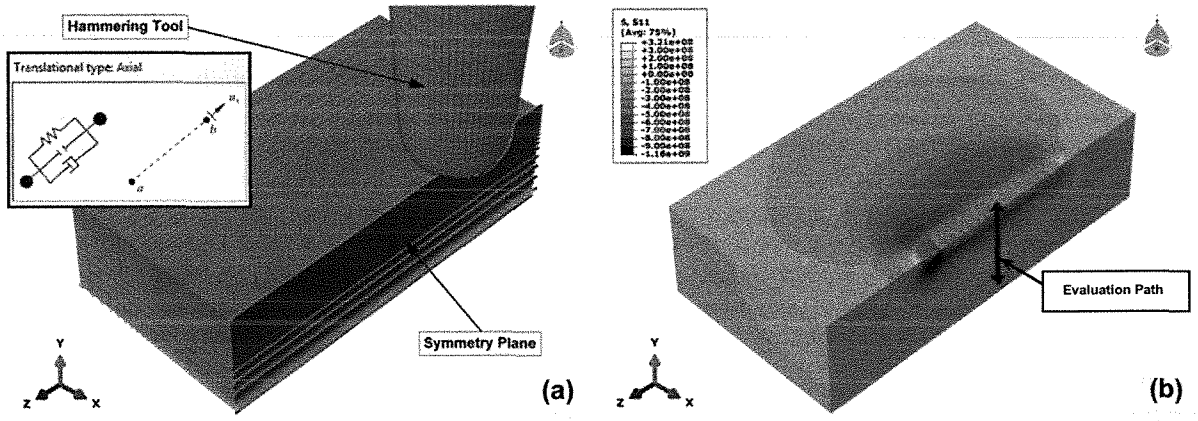

Figure 1: (a) FE-Model of specimen and hammering tool (b) Stress distribution after hammer peening

During the simulation the hammering tool was moved 6*mm* in the *z*-direction using a stepped amplitude (0.4*mm* infeed per step), while the hammering tool oscillates in the *y*-direction with constant frequency (*f*=100*Hz*) and amplitude *u*.

The considered material was a construction steel similar to *S355*, with an initial yield strength of σ_y=400*MPa* and an elastic modulus *E*=200*GPa*. For the investigation of the effects of some numerical features the strain rate dependence was neglected, assuming that it has no relevant influence in this context. The hammering process is considered isothermal.
The resulting residual stress depth profiles for the different mesh refinements (constant model features: indentation depth *u*=0.1*mm*, friction coefficient c_f=0.15, material with isotropic hardening without strain rate dependence) are shown in Figure 2 (a).

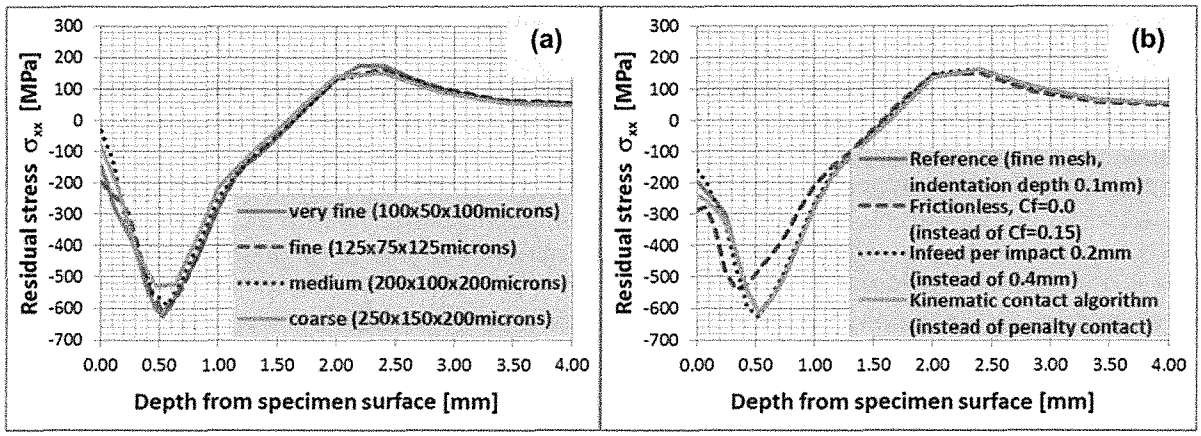

Figure 2: (a) Residual stress depth profiles for different mesh refinements (b) Residual stress depth profiles for different boundary conditions (fine mesh)

In general, the plastic deformation from hammering induces compressive residual stresses in the peened surface balanced by some tensile stress in the interior. Maximum compressive stresses of approximately 600*MPa* were determined. According to the Hertzian contact between the spherical tip of the pin and the plane plate, the maximum compressive stress was evaluated in a depth of approximately *0.50mm*. These results are in a good qualitative and quantitative agreement with experimental results and results from numerical studies [7].
Concerning the mesh dependence of the results, it becomes clear that the location of the maximum compressive stress is nearly equal for all mesh refinements and only the coarse mesh yields a differing value. Different stress results occur at the specimen surface, with the tendency to a higher compressive stress for the finer meshes. In summary, the fine mesh seems to be a good compromise between accuracy and numerical effort. Therefore, the fine mesh was used for all further simulations.

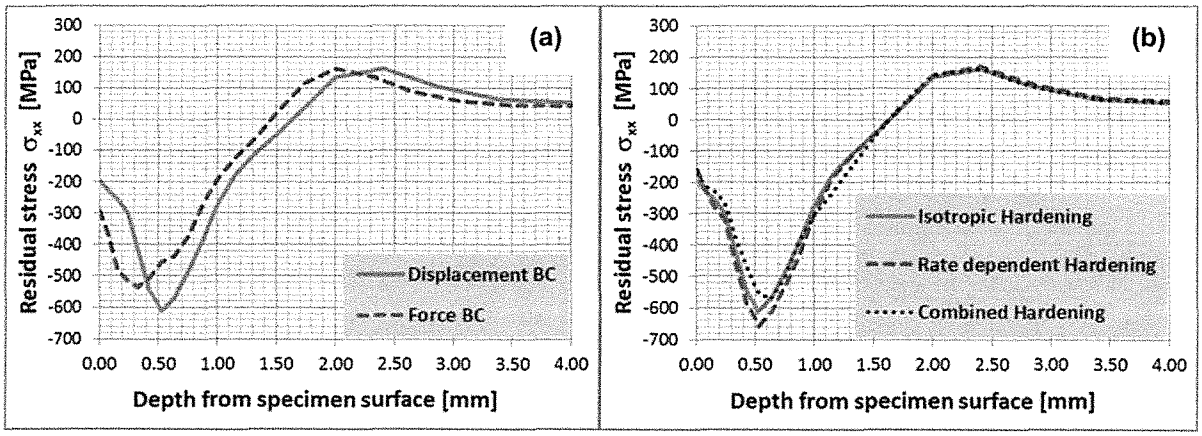

Figure 3: (a) Residual stress depth profiles for different loading boundary conditions (b) Residual stress depth profiles for different material models

The next investigated features were the influence of the friction coefficient, the overlap of the indentations (controlled by infeed per impact) and the contact algorithm for the normal to surface direction. The results are shown in Figure 2 (b) with the stress depth profile from the previous simulation (Fig. 2 (a), fine mesh) as reference. Changing the contact algorithm for the normal to surface direction from the penalty to the hard kinematic formulation affects the solution slightly nearby the specimen surface. A different movement of the hammering tool (infeed $0.2mm$ instead of $0.4mm$) has no significant influence on the stress depth profile. Thus, a step displacement of $0.4mm$ seems to be a good compromise between numerical calculation efforts and solution accuracy for this case. In contrast, a frictionless contact formulation considerably affects the stress depth profile, with a higher compressive stress at the surface and a lower peak value. Without appropriate experimental results, it is not possible to verify if this is a real or a (partial) numerical effect, but it definitely becomes clear that this feature must be handled with care at model definition.
Furthermore, the influence of the loading boundary conditions (BC) for the hammering tool and the effect of the material hardening behavior were investigated. The results are shown in Figure 3 (a) and 3 (b), respectively. Concerning the influence of the loading BC, it becomes clear that displacement BC (given indentation amplitude u) in general yield a different solution compared to force BC (accelerating force, controlled via a user subroutine) for a similar indentation depth. In this context, it must be mentioned that a specific indentation depth can be realized via different combinations of hammer mass and accelerating force. Therefore, the stress depth profile shown in Figure 3 (a) is only one possible variant, there may be variants closer to the displacement BC solution. Furthermore, strain rate effects on the material hardening behavior are neglected (for sake of simplicity; influence of material behavior is given in Figure 3 (b)). Nevertheless, for as much as possible realistic results force controlled BC may be beneficial.
The material hardening law features an observable effect on the stress depth profile; it mainly influences the peak value of the compressive residual stress. Figure 3 (b) compares the stress depth profile for an isotropic strain rate independent hardening law with the respective profiles for an isotropic strain rate dependent hardening law (Johnson Cook) and a mixed isotropic-kinematic (combined) strain rate independent hardening model (Chaboche-model). The combined hardening model includes softening of material after a change of the loading direction and provides a lower peak stress. The isotropic rate dependent hardening model respects the increase of the yield strength with increasing strain rate and provides a higher peak stress compared to the results for the isotropic strain rate independent hardening law. Due to the repeated impact of the hammering tool the elastic-plastic material undergoes a local hardening cycle. Thus, the combined hardening model should provide the most realistic results when it is enhanced by strain rate dependence.
The last investigated modelling feature was a technique for a rapid mesh coarsening outside the hammer peening process zone.

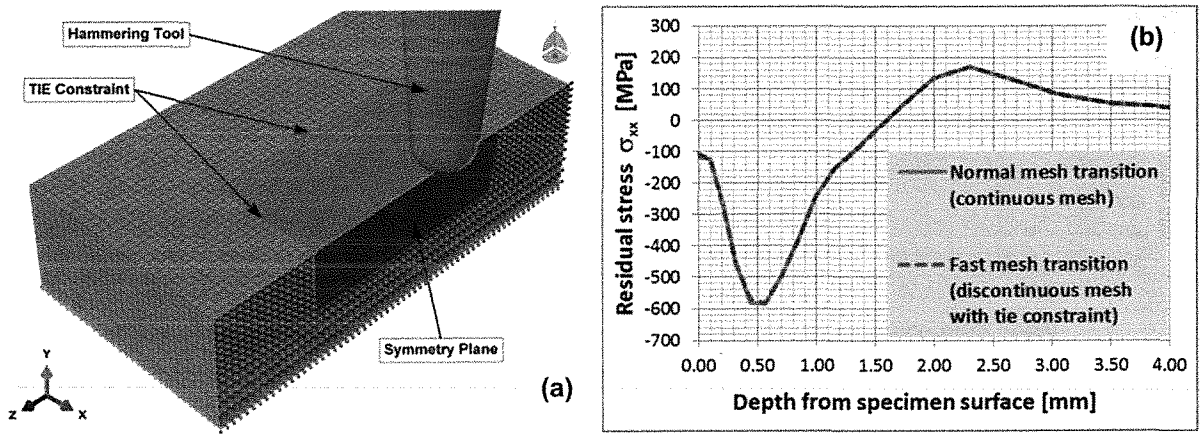

Figure 4: (a) FE-Model for rapid mesh transition (b) Residual stress depth profiles for different mesh transition techniques

A tie constraint constrains each of the nodes on the slave surface (fine) to have the same motion as the point on the master surface (coarse) to which it is closest and eliminates the degrees of freedom of the slave surface nodes. Figure 4 (a) shows the FE-Model for rapid mesh transition, while Figure 4 (b) contains the residual stress depth profiles for the different mesh transition techniques (normal transition means no tie constraint, i.e. a continuous mesh). As one can see, there is no observable difference between the stress depth profiles for the different mesh transition techniques. Thus, using the fast mesh transition the numerical effort can be reduced significantly without a relevant loss of accuracy. In the considered case, the runtime of the model with fast mesh transition is 50% lower.

Application to weld specimen

The welding process causes residual stresses in the structure, which are superimposed by the acting operational loads. Hence, the effective maximum local stress in the structure increases. Additionally, the weld toe topography represents a sharp notch. These phenomena cause a reduced fatigue life time of welded structures.

A half symmetrical (*y*-*z*-plane as symmetry plane) model of a welded specimen was used for the simulations. The length of the weld seam of the specimen is 25*mm*. The high frequency hammer peening treatment was applied onto the inner 20*mm* of the weld toe. The weld toe area requires a fine mesh because of the high local plastic deformations caused by the post-treatment. The welding residual stresses σ_{xx} perpendicular to the weld seam are shown in Figure 5 (a). The maximum values are located at the center of the welding line (z=12.5*mm*). The respective depth profile of the residual stresses is shown in Figure 6 (a).

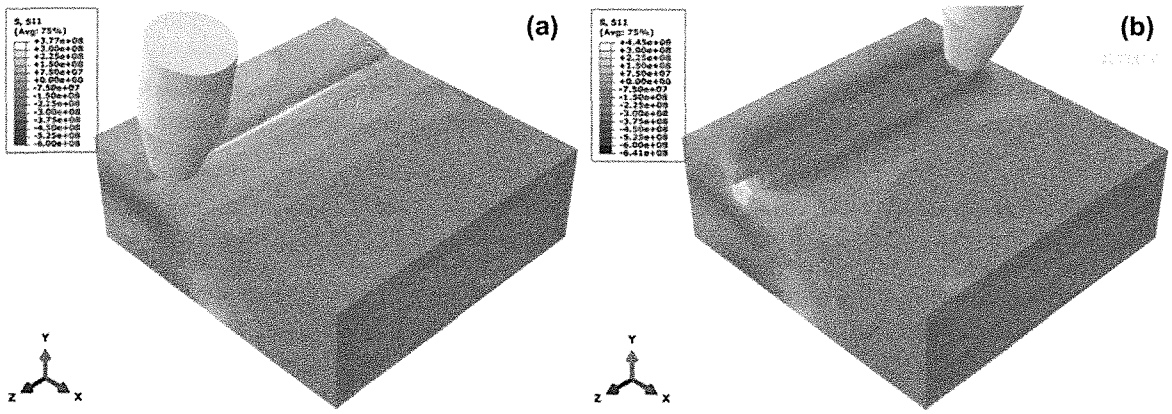

Figure 5: (a) Residual stress distribution after welding (b) Residual stress distribution after hammer peening

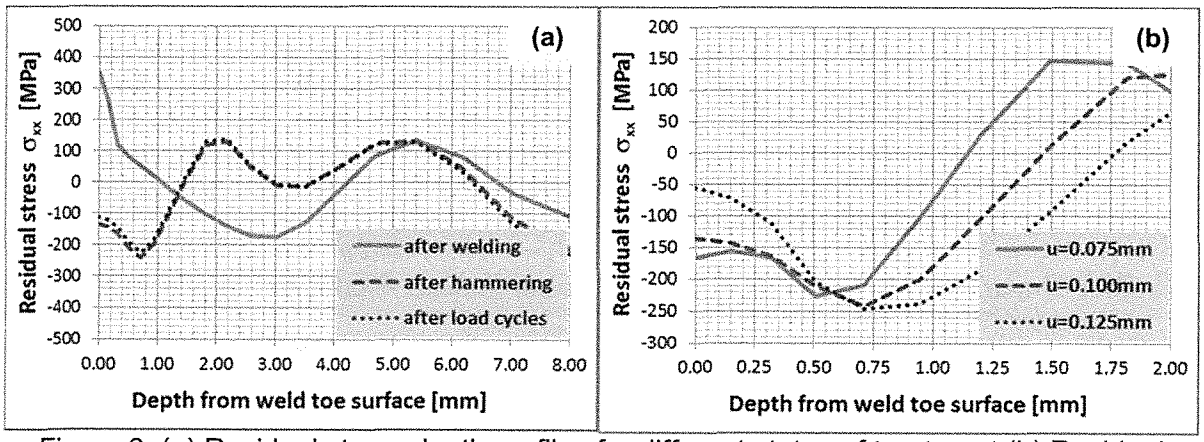

Figure 6: (a) Residual stress depth profiles for different states of treatment (b) Residual stress depth profiles [after hammering] for different process parameters [indentation depth *u*]

At the weld toe, a tensile residual peak stress of approximately 350*MPa* can be observed.
The results of the weld specimen (residual stress state, plastic strains) were imported into the FE-model for the simulation of the high frequency hammer peening treatment. The hammering tool was modelled with a tip radius of r=2*mm* and the specimen was supported using a rigid frame. The indenter was adjusted with an angle of 20° with respect to the specimen surface normal. The maximum axial amplitude of the hammering tool equaled 0.10*mm*. After each indentation, the hammering tool was moved 0.4*mm* along the weld toe.
Figure 5 (b) illustrates the result of the hammer peening treatment process by the change of the residual stresses distribution. The weld toe geometry is rounded out and reduces the notch effect, the top surface is work hardened and compressive residual stresses are induced by the treatment. Figure 6 (a) shows the depth profile of the residual stresses σ_{xx} (z=12.5*mm*). At the top surface, compressive residual stresses are induced up to a depth of approximately 1.5*mm*. Equilibrium conditions cause tensile residual stresses in the material below the treated volume. The FE-simulation enables a relatively easy execution of parameter studies. Figure 6 (b) illustrates the effect of a variation of the hammer peening intensity (indentation depth u). For the considered case, the initially chosen intensity (u=0.1*mm*) seems to be a good compromise with respect to the value and location of the maximum compressive residual stress and the compressive residual stress nearby the top surface.
Having determined the residual stresses after the hammer peening treatment, one can apply several load cycles to the specimen, in order to simulate the fatigue life tests applied to real specimens. These cycles had a constant stress range, with $\Delta\sigma_{xx\text{-load}}$=±300*MPa*. As one can see in Figure 6 (a), the residual stresses do not vanish despite a stress redistribution caused by the operational loads. Hence, the fatigue life can be improved by hammer peening.

Conclusions

Explicit simulations of the high frequency hammer peening treatment were performed using the software package *ABAQUS*. Possible effects of different numerical modelling features (mesh refinement, mesh transition, contact formulation, loading boundary conditions and material model) could be identified. Subsequently, the established modelling technique was successfully applied for the calculation of the residual stress field of a weld specimen after hammer peening treatment. Thus, the simulation technique established within the framework of this study provides the basis for a simulation loop including structural welding simulation, numerical simulation of the hammer peening process, and finally, an estimation of the fatigue life of the structure.

References

[1] E. Statnikov, V. Trufyakov, P. Mikheev, Y. Kudryavtsev, *Specification for weld toe improvement by ultrasonic impact treatment*, International Institute of Welding, Paris (1996) [IIW Document XIII-1617-96].

[2] H.C. Yildirim, G.B. Marquis, Z. Barsoum, *Fatigue assessment of high frequency mechanical impact (HFMI)-improved fillet welds by local approaches*, International Journal of Fatigue, Vol. 52 (2013), pp 57-67.

[3] H.C. Yildirim, G.B. Marquis, *Fatigue strength improvement factors for high strength steel welded joints treated by high frequency mechanical impact*, International Journal of Fatigue, Vol. 44 (2012), pp 168–76.

[4] G. B. Marquis, E. Mikkola, H. C. Yildirim, Z. Barsoum, *Fatigue Strength Improvement of Steel Structures by High-Frequency Mechanical Impact: Proposed Fatigue Assessment Guidelines*, Weld. World, Vol. 57 (2013), pp 803–822.

[5] P. J.Haagensen, S. J. Maddox, *IIW Recommendations on post weld improvement of steel and aluminum structures*, IIW Document XIII-2200r4-07, revised February 2010.

[6] R. Baptistaa, V. Infante, C. Branco, *Fully Dynamic Numerical Simulation of the Hammer Peening Fatigue Life Improvement Technique*, Procedia Engineering Vol. 10 (2011) pp 1943–1948.

[7] D. Simunek, M. Leitner, M. Stoschka, *Numerical simulation loop to investigate the local fatigue behaviour of welded and HFMI-treated joints*, IIW Document XIII-WG2-136-13.